Available online at www.sciencedirect.com
ScienceDirect
Journal of Hazardous Materials 150 (2008) 394–400
Journal of Hazardous Materials
www.elsevier.com/locate/jhazmat

Effect of sintering temperature on the characteristics of sludge ceramsite

G.R. Xu *, J.L. Zou, G.B. Li

School of Municipal and Environmental Engineering, Harbin Institute of Technology, P.O. Box 2602, Harbin, Heilongjiang Province, China

Received 23 December 2006; received in revised form 15 April 2007; accepted 26 April 2007
Available online 3 May 2007

Abstract

In order to investigate the effect of sintering temperature on the characteristics of sludge ceramsite and find an optimal sintering temperature, dried sewage sludge, clay, and water glass were mixed at ratios of dried sewage sludge/clay = 33% and water glass/clay = 15%. Then these mixtures were heated to 850, 900, 950, 1000, 1100, and 1200 °C for production of sludge ceramsite. The sludge ceramsite were characterized by DTA-TGA, SEM-EDS, XRD, and XRF. The results indicate that the differences in thermal behaviours are caused by the compositional and structural variations; the ceramsite sintered at 1000 °C has more uniformly distributed finer pores (0.5 μm < pore size < 10.0 μm), while the ceramsite sintered at other temperatures has less pores and rougher surfaces. The main crystalline phases of ceramsite are quartz and kyanite below 1000 °C; kyanite is the main crystalline phase at 1000 and 1100 °C, and most of the crystalline phases are mullite at 1200 °C. It is therefore concluded that sintering temperature has a significant effect on the characteristics of sludge ceramsite, and that 1000 °C is the optimal sintering temperature.

Keywords: Sludge ceramsite; Crystalline phase; Sintering temperature; Thermal behaviour

1. Introduction

Due to rapid urbanization and implementation of more stringent effluent criteria in recent years, sewage sludge is now being generated in an ever-increasing amount. While conventional disposal options, such as landfill, application to farmland and forestry, incineration, and sea dumping are used to treat sewage sludge [1,2], its high content of organic substances has caused much concern about leachate contamination, and these organic matters may lead to excessive propagation of microorganisms [3–5], and so the ultimate disposal of excess sludge has been and continues to be one of the most expensive problems encountered by wastewater utilities, e.g. the treatment of excess sludge may account for 25–65% of the total plant operation cost [6]. Stringent environmental legislation has caused dramatic change in ways and means used to dispose sludge [7]. For example, sewage sludge could be directly used in agriculture as fertilizer a few years ago, but this is now hampered by the legal criteria for its high content of heavy metals [8].

Another frequently used method for disposal of sludge is thermal treatment [9–13], which involves incineration, gasification, and pyrolysis. It is now generally accepted that sewage sludge is a resource with much potential for beneficial applications other than direct disposal and it can be used for production of activated carbon through pyrolysis under controlled conditions and/or through chemical treatment. Several recent investigations show the feasibility of this conversion because almost any carbonous material can be used as a precursor for preparation of activated carbons [14–16].

Solidification/stabilization (S/S) technologies (disinfections, reduction of leaching of heavy metals, decomposition/stabilization of persistent organic compounds, etc.) are the processes designed to improve waste-handling, decrease the surface area to inhibit heavy metals from being transferred or leached, reduce the solubility of contaminant compounds, and detoxify hazardous constituents [12,17]. They are widely used for treating both inorganic and organic waste materials. Some work has been done on the special properties of glass–ceramics made from sewage sludge ash [3,18]. Sewage sludge ash has been compacted and heated at different temperatures to produce a range of sintered ceramic materials [19,20]. In addition to the silicon and aluminum-rich characteristics, sewage sludge also exhibits a significant specific surface area and cation-exchange capacity. The conversion of sewage sludge into lightweight aggregates for production of concrete has been investigated by several researchers [21,22]. Properties of lightweight sludge ash

* Corresponding author. Tel.: +86 45186282559; fax: +86 45186282559.
E-mail address: xgr@hit.edu.cn (G.R. Xu).

0304-3894/$ – see front matter © 2007 Elsevier B.V. All rights reserved.
doi:10.1016/j.jhazmat.2007.04.121

Table 1
General physicochemical characteristics of clay

Chemical composition (wt.%)								
SiO_2	Al_2O_3	Fe_2O_3	TiO_2	K_2O	Na_2O	CaO	MgO	H_2O
≤65.0	≥25.0	≤2.5	≤1.2	≤1.2	<0.4	<0.5	<0.5	<10.0

Physical properties			
Particle size (μm)	Plastic index	Linear shrinkage (%)	Moisture (%)
>5	4.0	8.5–12.0	≤15.0

aggregates were also investigated by Bhatty and Reid [23], who reported concrete with moderate strength could be produced by using pelletized or slabbed lightweight coarse aggregates sintered at a temperature between 1050 and 1110 °C.

A new effective approach to the usage of sewage sludge is to produce lightweight ceramsite. Ceramsite, which contains inorganic components, such as $A_{l2}O_3$, SiO_2, Fe_2O_3, FeO, CaO, MgO, Na_2O, and K_2O, has been used as construction materials, for example cement mortars, concrete mixtures, bricks, as fine aggregate in mortars and ceramic materials, or as filter media in reactors for treating municipal/industrial wastewater/secondary effluent in wastewater treatment plants [24]. Desirable properties can be achieved by controlling the initial ceramsite composition and applying a suitable heat treatment. This study aims at the preparation of suitable sludge ceramsite used as filter media with significant specific surface area and coarse surface.

As an artificial lightweight aggregate, the production of sludge ceramsite involves the processes of bloating and sintering during heat treatment. The main purpose of the present work is to investigate the influence of different sintering temperatures on the characteristics of sludge ceramsite made with dried sewage sludge as an additive, and to find an optimal sintering temperature for ceramsite, as well as to establish effective parameters for evaluation.

2. Materials and methods

The ceramsite under study was made of (1) clay as the skeletal material with physicochemical characteristics as shown in Table 1; (2) water glass Na_2SiO_3 with modulus of 3.2; (3) dried sewage sludge with chemical characteristics as shown in Table 2. Wet sewage sludge was obtained from lab's activated sludge reactor used for treating domestic wastewater, and dried sewage sludge was made by drying it at 105 °C until it reached invariable mass. Dried sewage sludge consisted of 35% inorganic matter in the forms of metal and non-metalic oxide and salt, and 60% organic matter in the form of dead bio-solid and 5% water content. Dried sewage sludge, clay, and water glass are the initial raw materials for ceramsite production and the optimal ratios of dried sewage sludge/clay, and water glass/clay are 33 and 15%, respectively [24]. These three raw materials were mixed using YK-60 pelletizing machine (made in China) to pelletize raw ceramsite with particle sizes of 5–8 mm and the samples were dried at 110 °C in a blast roaster for 24 h. The heating of samples started at 20 °C, heated at a rate of 8 °C/min in a muffle furnace, and the samples were soaked at 200, 550, 800 °C, and preset temperature for a duration of 10 min, and then these were naturally cooled until they reached room temperature.

Powder XRD patterns of ceramsite were recorded on a D/max-γ β X-ray diffractometer with 50 mA and 40 kV, Cu Kα radiation. Major elements of ceramsite were analysed using a Philips PW 4400 XR spectrometer (XRF). SEM-EDS analyses were conducted using S-570 scanning electron microscope and TN-5502 X-ray energy dispersive spectrum. The thermal behaviours of samples were examined by DTA-TGA using a ZRY-2P simultaneous DTA-TGA analyser while the samples were heated at a rate of 8 °C/min from 20 to 1150 °C in air. Samples weighed from 4 to 10 mg in mass, and they were put into a Pt–Rh crucible with 20 taps. All curves were evaluated using the TA-instruments software. The second derivative differential thermal curve was used for determination of peak temperature.

3. Results and discussion

3.1. Thermal behaviour analyses

The thermal behaviours of the raw material mixtures (clay, dried sewage sludge, water glass) is examined by DTA-TGA and compared with the thermal behaviours of clay alone, dried sewage sludge alone, and their mixture mixed at a ratio of sludge/clay = 33 wt.%.

It can be seen from Fig. 1 that the DTA curve of clay does not change much from 20 to 463.2 °C and has little weight loss in TG analysis. An endothermal change is observed in DT analysis from 463.2 to 524 °C with 4.9% weight loss. Exothermal change is observed in DT analysis from 700.1 to 899 °C with 0.82%

Table 2
Chemical components analyses of dried sewage sludge (wt.%)

Chemical components analyses								
SiO_2	Al_2O_3	Fe_2O_3	CaO	MgO	P_2O_5	K_2O	Others	Carbonaceous matter
16.28	6.35	5.15	4.10	1.67	1.65	1.12	<0.89	<62.90

Chemical elements analyses								
Zn	Fe	Mn	Si	Cu	Ca	Mg	Co	Cr
0.19	4.30	0.17	16.3	0.045	4.14	1.58	<0.01	0.034
P	Na	K	Al	Ni	C	S	N	Others
1.25	0.56	1.15	6.66	0.22	61.20	0.06	1.55	<0.60

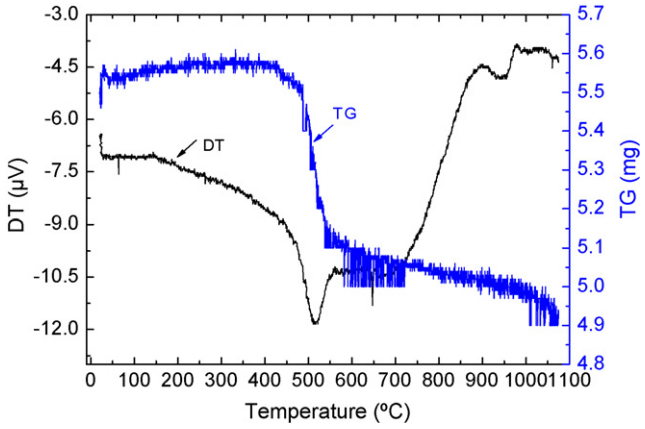

Fig. 1. DT and TG analyses of clay.

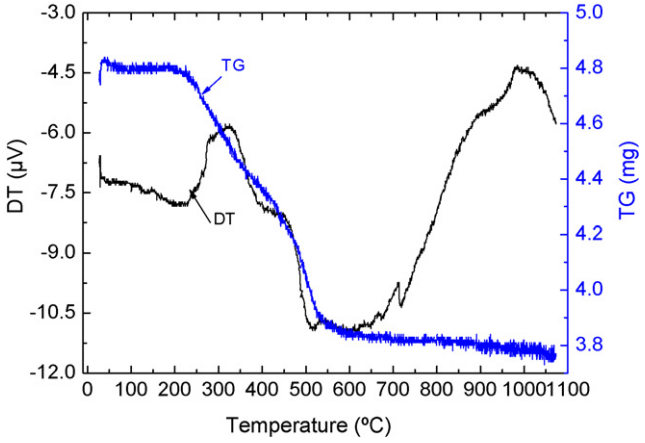

Fig. 3. DT and TG analyses of mixture of clay and sludge (sludge/clay of 33%).

weight loss and from 942 to 990 °C with 0.72% weight loss, respectively. The weight loss fluctuates as investigated in TG analysis due to silicate hydrates gradually dehydrating and it is also reported that silicate hydrates dehydrate gradually over a wide temperature range up to 800 °C [25].

The exothermic peaks, endothermic peaks, and corresponding weight losses of sludge shown in Fig. 2 are due to an exothermic change at a temperature in the range of 87–327.7 °C, dehydration of silicate hydrates, and release of CO with 32.2% weight loss; an endothermic change at a temperature in the range of 327.7–399.8 °C, reaction of carbonous materials with 11.3% weight loss; an exothermic change at a temperature in the range of 399.8–482 °C, the release of CO_2 with 14.6% weight loss; an endothermic change at a temperature in the range of 482–1100 °C, some phase changes, and formation of crystalline phases with 12.2% weight loss.

It can be seen from Fig. 3 that thermogravimetric (TG) and differential thermal (DT) plots of the mixture of clay and sludge are closely interrelated. DT diagrams for mixture of clay and sludge show an endothermic peak at 215 °C, due to evaporation of adsorbed water. Exothermic peak signals at 315.3 °C correspond to H_2O loss from the mixture of clay and sludge. The deep peak at 601 °C, corresponding to the decomposition of carbonous materials, is associated with 20.1% weight loss in TG analysis.

The thermal analysis of the mixture of clay, sewage sludge, and water glass at ratios of dried sewage sludge/clay = 33% and water glass/clay = 15% indicates that there is a substantial weight loss at 530 °C indicated by a definite endothermic peak, which suggests the decomposition of carbonous materials as shown in Fig. 4 and with the weight loss of 18.8% in TG analysis. Endothermic change is observed from 286.3 to 1100 °C in macroscopic view, which should be attributed to the crystallization of mullite, quartz, kyanite, etc., but probably sometimes the exothermic and endothermic reactions are interchanged from 286.3 to 1100 °C in microscopic view.

The differences in thermal behaviours of the four samples (Figs. 1–4) are due to the changes in compositions and structures of the mixtures [25]. The formation of crystals is accompanied by relatively abundant glassy phases at a temperature above 950 °C [18]. And the eutectic point of the mixture can be reduced by the reaction of water glass and air ($Na_2O{\cdot}nSiO_2{\cdot}xH_2O + CO_2 \rightarrow Na_2CO_3 + nSiO_2 + xH_2O\uparrow$), and by the dispersion of alkali metal oxide (i.e. Na_2O, etc.) originating from the decomposition of Na_2CO_3 ($Na_2CO_3 \rightarrow Na_2O + CO_2\uparrow$) in the heating process. This

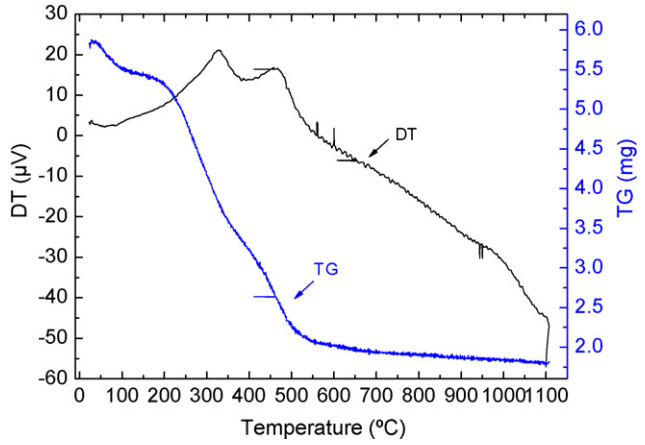

Fig. 2. DT and TG analyses of sludge.

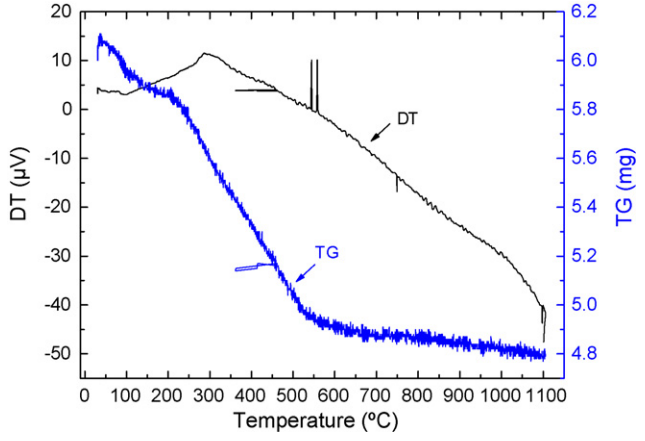

Fig. 4. DT and TG analyses of mixture of clay, sludge, and water glass (sludge/clay of 33% and water glass/clay of 15%).

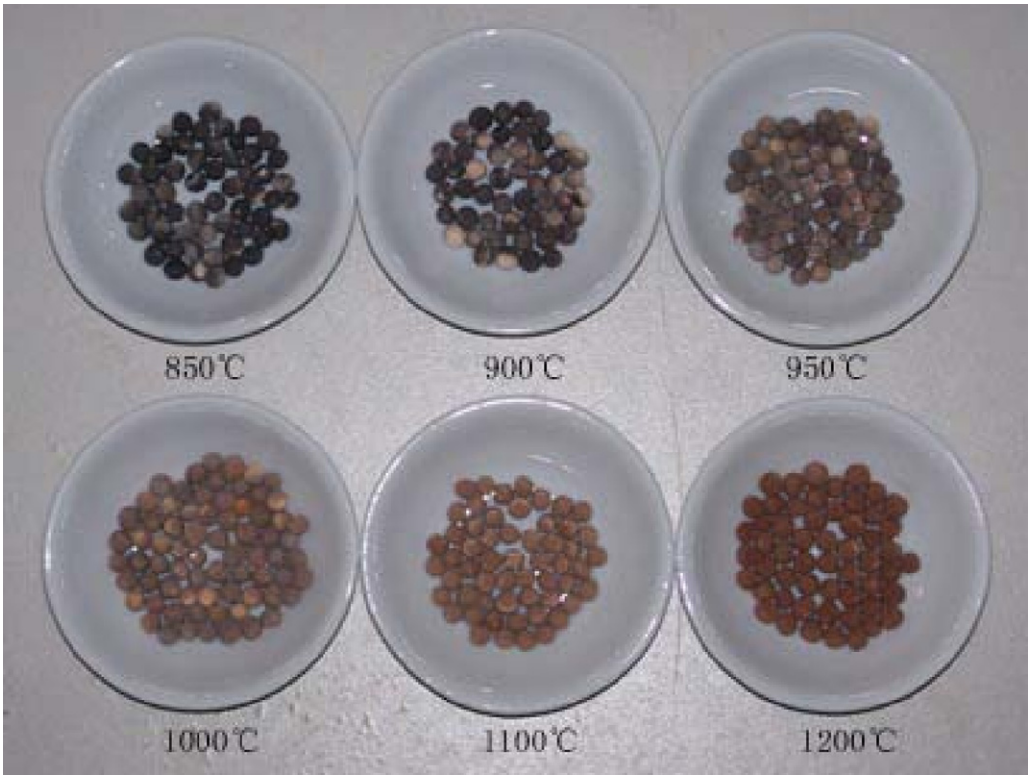

Fig. 5. Pictures of sludge ceramsite sintered at 850, 900, 950, 1000, 1100, and 1200 °C.

is the reason why water glass was added as a component in the sludge ceramsite making process [24]. 950–1100 °C can be considered as the optimal range of eutectic point for the mixture.

3.2. Morphological structures analyses

The appearance of sludge ceramsite sintered at different sintering temperature (850, 900, 950, 1000, 1100, and 1200 °C) was shown in Fig. 5. It can be seen from the photograph that the colours of the samples are different from each other changing from dark to wine-coloured. Then the samples were gilt with porous Pt and their surface morphology was examined by SEM-EDS.

As shown in Table 3, Na, Al, Si, K, Ca, Ti, and Fe are all detectable on the surface of ceramsite. There are some differences in the contents of detectable elements on the surface of ceramsite sintered at different temperatures. The contents of Si and Al are higher at a temperature below 1000 °C, and those of Fe, Ca, Ti, K, and Na are higher at a temperature above 950 °C, which suggests that the kinetics of reaction of glassy phases may be higher near the quartz (SiO_2) or kyanite (Al_2SiO_5) grains, and its viscosity may be lower in comparison with the glass embedded in the mullite ($Al_2O_3{\cdot}SiO_2$)-rich zone. The results indicate sintering temperature has a significant effect on the distribution of elements in ceramsite.

Table 3
Elementary analysis on surface of ceramsite (wt.%)

Sintering temperature (°C)	Elements						
	Al	Si	K	Ca	Ti	Fe	Na
850	12.21	65.05	3.39	1.11	4.23	14.00	–
900	14.15	62.92	3.75	2.27	2.84	14.07	–
950	11.84	62.23	3.46	2.28	2.61	16.05	1.51
1000	11.78	44.99	4.68	6.97	4.08	25.78	1.71
1100	11.34	46.24	4.22	6.87	3.54	26.00	1.79
1200	12.18	50.59	4.10	5.97	4.18	21.36	1.61

EDS analyses show that quartz content decreases in the range of sintering temperature (850–1200 °C) as other crystals form just under the surface of the ceramsite and quartz species go further under the surface of the ceramsite, which indicates that sintering temperature has a significant effect on crystalline phase of ceramsite.

It can be seen from Fig. 6(a, 850 °C) that the enrichment of quartz on the surface of ceramsite is accompanied by rough surfaces and big pores. This phenomenon occurs due to the sintering temperature (850 °C) being relatively low for the production of ceramsite. Fig. 6(b, 900 °C) shows that there are a large number of quartz crystals on the surface of ceramsite and kyanite crystals in a subsurface region of ceramsite and an intermediate region with less albite ($NaAlSi_3O_8$) between quartz and kyanite crystals, and that is where an incomplete-glassy phase is embedded.

It can be seen from Fig. 6(c, 950 °C) that the surface structure of ceramsite is very rough and has tiny pores, and the microstructure of ceramsite consists of a network of quartz crystals embedded in an incomplete-glassy phase. The reason may

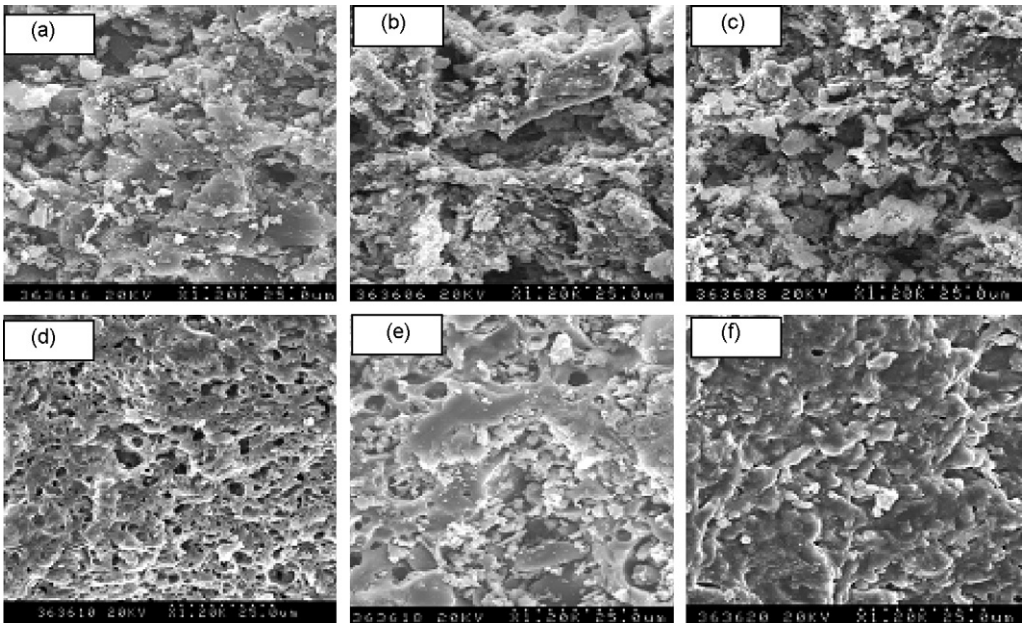

Fig. 6. Scanning photomicrographs of ceramsite surface at 850, 900, 950, 1000, 1100, and 1200 °C.

be that the formation of a bubbled microstructure due to the softening of the glassy phase together with evolution of gases generated by the decomposition of inorganic phases appears within the material [20]. The coarsening of quartz crystals as sintering temperature increases is one of the detectable characteristics of ceramsite, and totally different microstructures of ceramsite can be observed at a sintering temperature above 950 °C.

It can be clearly seen from Fig. 6(d, 1000 °C) that there is a matrix containing a large number of isolated, approximately spherical pores, typically 0.5–10 μm in diameter. The microstructure of ceramsite has more uniformly distributed small pores (0.5 μm < pore size < 10.0 μm), interconnected with quartz and other crystals. It could be explained that the pores form as the residual glassy phase viscosity falls to a level when gas-forming inorganic decomposition reactions can produce the observed pores [26].

It can be seen from Fig. 6(e, 1100 °C) that the densely compacted microstructures in ceramsite are due to the formation of glassy phases at 1100 °C. The decrease in the viscosity of glassy phase in the region enhances the diffusion of kyanite species from the subsurface region to the upper surface region.

Irregular crystals form at 1100 °C as shown in Fig. 6(e) while relatively regular crystals of glassy structures crystallize at 1200 °C as shown in Fig. 6(f). The relatively low-density ceramsite produced by heating at 1200 °C appears to be hard and has a glassy surface. However, it is still an open question as to why this crystallization process of mullite occurs in the surface of ceramsite. It seems to be reasonable to assume that most of the volatile components (carbonate and alkaline oxides) of glassy phases tend to evaporate from the surface of ceramsite, thereby, originating a gradient concentration of crystals that may be favourable to the nucleation of mullite in this region.

3.3. Crystalline phases and chemical composition analyses

The crystalline phases of ceramsite sintered at different sintering temperature (850, 900, 950, 1000, 1100, and 1200 °C) are as shown in Table 4. Although the analysis was conducted using an XRD pattern database (International Centre for Diffrac-

Table 4
Crystallographic and glass phases in sludge ceramsite

Sintering temperature (°C)	Major constituents	Minor constituents
850	Quartz (SiO_2)	Anorthoclase ((Na, K)$AlSi_3O_8$)
	Kyanite (Al_2SiO_5)	
900	Quartz (SiO_2)	Albite ($NaAlSi_3O_8$)
	Kyanite (Al_2SiO_5)	
	Sodium silicate ($Na_2Si_2O_5$)	
950	Quartz (SiO_2)	Mullite ($Al_2O_3{\cdot}SiO_2$)
	Kyanite (Al_2SiO_5)	
1000	Kyanite (Al_2SiO_5)	Mullite ($Al_2O_3{\cdot}SiO_2$)
	Quartz (SiO_2)	Sillimanite (Al_2SiO_5)
	Albite ($NaAlSi_3O_8$)	
1100	Kyanite (Al_2SiO_5)	Mullite ($Al_2O_3{\cdot}SiO_2$)
	Albite ($NaAlSi_3O_8$)	
	Quartz (SiO_2)	
1200	Mullite ($Al_2O_3{\cdot}SiO_2$)	Albite ($NaAlSi_3O_8$)
	Quartz (SiO_2)	Sillimanite (Al_2SiO_5)
	Kyanite (Al_2SiO_5)	

Table 5
Chemical components analyses of ceramsite sintered at 1000 °C (wt.%)

SiO_2	Al_2O_3	Na_2O	Fe_2O_3	P_2O_5	CaO	TiO_2
64.46	19.52	6.98	2.41	2.23	1.23	1.14
K_2O	MgO	ZnO	MnO	CuO	BaO	
1.03	0.59	0.09	0.04	0.03	0.03	

tion Data, ICDD), no other crystalline phases matched sufficient peaks to be positively identified. The major crystalline phase at 850 °C is quartz (SiO_2) and kyanite (Al_2SiO_5) as shown in Fig. 7. Mullite ($Al_2O_3{\cdot}SiO_2$, mullite 1:1), quartz (SiO_2) and kyanite (Al_2SiO_5) are the main crystalline phases of ceramsite at 1200 °C as shown in Fig. 7(f).

The changes in crystallization temperature do not have any effect on the formation of crystals and the major crystalline phases remain almost unchanged as shown in Fig. 7(a–c). It can be also seen from Fig. 7 that no major crystalline transformation and/or crystalline phase occur at a sintering temperature below 1000 °C, and quartz (SiO_2) and kyanite (Al_2SiO_5) are the main crystals.

The amount of mullite increases until it becomes a major crystalline phase as sintering temperature increases as shown in Fig. 7(d–f). Kyanite crystals are major crystalline phases when the crystallization temperatures are 1000 and 1100 °C, and a major portion of crystals is mullite crystal at 1200 °C. The microstructures of ceramsite sintered at 1200 °C also confirm the formation of several indistinct crystalline phases in ceramsite as shown in Fig. 6(f).

Mullite has already been formed at 950 °C, as one of minor crystalline phases, co-existing with quartz and a small amount of kyanite. As the sintering temperature increases, the intensity of XRD peaks of mullite increases, while other crystalline phases tend to decrease. As the total amount of quartz decreases, albite and mullite derived from kyanite dissolution either remain in glassy phase or are used to nucleate other crystals in ceramsite at a sintering temperature above 950 °C. Accordingly, although these crystalline phases (mullite 1:1, quartz, and kyanite) appear at 1200 °C, there is still the residual of albite in ceramsite as shown in Fig. 7(f).

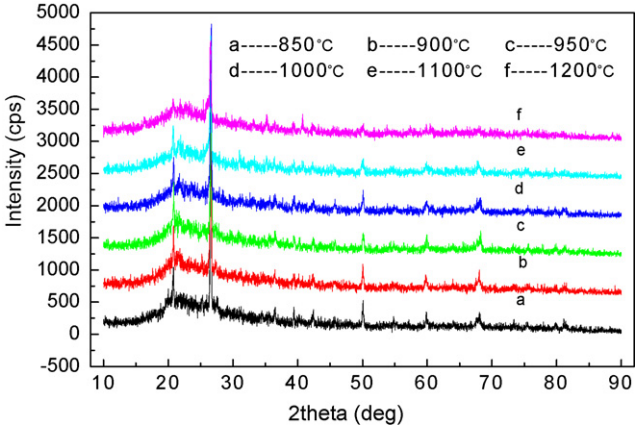

Fig. 7. XRD patterns of ceramsite at 850, 900, 950, 1000, 1100, and 1200 °C.

It can be seen from the results above that the main crystalline phases of ceramsite almost do not change in the range of 1000–1100 °C and kyanite, quartz, and albite are the main crystalline phases of ceramsite at both 1000 and 1100 °C. The morphological structure of ceramsite sintered at 1000 °C is better than that of ceramsite sintered at 1100 °C, so taking cost-saving and lower energy consumption into account, 1000 °C can be considered as the optimal sintering temperature for using dried sewage sludge as an additive to make ceramsite. Chemical composition of the ceramsite sintered at 1000 °C is analysed by XRF and tabulated in Table 5.

4. Conclusions

Differences in thermal behaviours are caused by different silicate contents and structures of the mixtures, and the mixture of clay, sewage sludge, and water glass mixed at the ratios of dried sewage sludge/clay = 33% and water glass/clay = 15% has the appropriate physical and chemical properties for the production of ceramsite. Glassy and liquid phases occur at a temperature above 900 °C because the transformation of fine quartz particles and presence of alkaline silicates in ceramsite enhance the reaction kinetics and increase chemical communication during the sintering reaction stage of ceramsite. Temperature of 1000 °C is appropriate for the production of sludge ceramsite and the samples prepared can satisfy the requirements for filter media used for water/wastewater treatment. It also indicates that ceramsite made with sewage sludge, as an additive is a comparatively sustainable sludge disposal application.

References

[1] X.G. Chena, S. Jeyaseelana, N. Graham, Physical and chemical properties study of the activated carbon made from sewage sludge, Waste Manage. 22 (7) (2002) 755–760.
[2] M. Otero, F. Rozada, L.F. Calvo, A.I. Garcĭıa, Elimination of organic water pollutants using adsorbents obtained from sewage sludge, Dyes Pigm. 57 (1) (2003) 55–65.
[3] H. Endo, Y. Nagayoshi, K. Suzuki, Production of glass ceramics from sewage sludge, Water Sci. Technol. 36 (11) (1997) 235–241.
[4] R. Kikuchi, Vitrification process for treatment of sewage sludge and incineration ash, J. Air Waste Manage. Assoc. 48 (11) (1998) 1112–1115.
[5] M. Otero, F. Rozada, L.F. Calvo, A.I. Garcĭıa, Kinetic and equilibrium modelling of the methylene blue removal from solution by adsorbent materials produced from sewage sludges, Biochem. Eng. J. 15 (1) (2003) 59–68.
[6] Q.L. Zhao, G.J. Kugel, Thermophilic/mesophilic digestion of sewage sludge and organic waste, Environ. Sci. Health 31 (1997) 2211–2231.
[7] Y. Liu, Chemically reduced excess sludge production in the activated sludge process, Chemosphere 50 (1) (2003) 1–7.
[8] A.H. Veeken, H.V. Hamelers, Removal of heavy metals from sewage sludge by extraction with organic acids, Water Sci. Technol. 40 (1) (1999) 129–136.

[9] L. Qiao, G. Ho, The effect of clay amendment on speciation of heavy metals in sewage sludge, Water Sci. Technol. 34 (7-8) (1996) 413–422.
[10] R. Cenni, F. Frandsen, T. Gerhardt, H. Spliethoff, Study on trace metal partitioning in pulverized combustion of bituminous coal and dry sewage sludge, Waste Manage. 18 (6-8) (1998) 433–444.
[11] W. Krebs, R. Bachofen, H. Brandl, Growth stimulation of sulfur oxidizing bacteria for optimization of metal leaching efficiency of fly ash from municipal solid waste incineration., Hydrometallurgy 59 (2-3) (2001) 283–290.
[12] A. Obrador, M.I. Rico, J.M. Alvarez, J. Novillo, Influence of thermal treatment on sequential extraction and leaching behaviour of trace metals in a contaminated sewage sludge, Bioresour. Technol. 76 (3) (2001) 259–264.
[13] K.S. Wang, K.Y. Chiang, C.C. Tsai, C.J. Sun, C.C. Tsai, K.L. Lin, The effects of $FeCl_3$ on the distribution of the heavy metals Cd, Cu, Cr, and Zn in a simulated multimetal incineration system, Environ. Int. 26 (4) (2001) 257–263.
[14] S. Jeyaseelan, G. Lu, Development of adsorbent/catalyst from municipal wastewater sludge, Water Sci. Technol. 34 (3/4) (1996) 499–505.
[15] M.J. Martŭın, M.D. Balaguer, M. Rigola, Feasibility of activated carbon production from biological sludge by chemical activation with $ZnCl_2$ and H_2SO_4, Environ. Technol. 17 (6) (1996) 667–672.
[16] L.F. Calvo, M. Otero, A. Morán, A.I. Garcĭıa, Upgrading sewage sludges for adsorbent preparation by different treatments, Bioresour. Technol. 80 (2) (2001) 143–148.
[17] A. Andrés, R. Ibáñez, I. Oritiz, J.A. Irabien, Experimental study of the waste binder anhydrite in the solidification/stabilization process of heavy metal sludges, J. Hazard. Mater. 57 (1-3) (1998) 155–168.
[18] J.P. Young, O.M. Soon, H. Jong, Crystalline phase control of glass ceramics obtained from sewage sludge fly ash, Ceram. Int. 29 (2) (2003) 223–227.
[19] N.R. Khalili, J.D. Vyas, W. Weangkaew, S.J. Westfall, S.J. Parulekar, R. Sherwood, Synthesis and characterization of activated carbon and bioactive adsorbent produced from paper mill sludge, Sep. Purif. Technol. 26 (2-3) (2002) 295–304.
[20] C.R. Cheeseman, C.J. Sollars, S. McEntee, Properties, microstructure and leaching of sintered sewage sludge ash, Resour. Conserv. Recycl. 40 (1) (2003) 13–25.
[21] C.C. Tsai, K.S. Wang, I.J. Chiou, Effect of SiO_2–Al_2O_3-flux ratio change on the bloating characteristics of lightweight aggregate material produced from recycled sewage sludge, J. Hazard. Mater. B134 (2006) 87–93.
[22] C. Collivignarelli, S. Sorlini, Reuse of municipal solid wastes incineration fly ashes in concrete mixtures, Waste Manage. 22 (2002) 909–912.
[23] J.I. Bhatty, K.J. Reid, Moderate strength concrete from lightweight sludge ash aggregates, Cem. Compos. Lightweight Concr. 11 (1989) 179–187.
[24] G.R. Xu, J.L. Zou, Y. Dai, Utilization of dried sludge for making ceramsite, Water Sci. Technol. 54 (9) (2006) 69–79.
[25] D.S. Klimesch, A. Ray, DTA-TGA of unstirred autoclaved metakaolin–lime–quartz slurries. The formation of hydrogarnet, Thermochim. Acta 316 (2) (1998) 149–154.
[26] V. Ducman, A. Mladenovic, J.S. Suput, Lightweight aggregate based on waste glass and its alkali–silica reactivity, Cem. Concr. Res. 32 (2) (2002) 223–226.